Tetranuclear organometallic complexes based on 1,2-ethanedithiolate ligands as potential precursors for $CuMS_2$ (M = Ga, In)

Dirk Friedrich, Oliver Kluge, Marcus Kischel and Harald Krautscheid[a]

[a] *Universität Leipzig, Institut für Anorganische Chemie, Johannisallee 29, 04103 Leipzig, Germany. Fax: 0049 34197 36199; Tel: 0049 34197 36172; E-mail: krautscheid@rz.uni-leipzig.de*

1 Supplementary information

1.1 Experimental

1.1.1 Starting material

$[(^{i}Pr_3PCu)_4(SCH_2CH_2S)_2]$ (1)

Under nitrogen atmosphere 1.7 g (12 mmol) of Cu_2O are suspended in a mixture of 20 ml of dry toluene and 10 ml of dry pyridine. 5 ml (26 mmol) of $P^{i}Pr_3$ and 1 ml (12 mmol) of $HSCH_2CH_2SH$ are added while stirring. The brick red suspension is heated to reflux. After 10 min the yellow solution is decanted and allowed to cool down to room temperature. After layering with 50 ml of *n*-heptane and storing at room temperature over night (12 hours), colorless crystals are formed. To assure completeness of crystallization the solution is stored at 2 °C for another 3 days. Now the yellow mother liquor is decanted, the crystalline solid is washed with *n*-heptane and dried in vacuo. Yield: 4.6 g (81 %). ^{1}H-NMR (C_6D_6, 400 MHz) δ_H in ppm: 3.10 (8H, s, br, ethylene), 1.84 (12H, pseudo-octet, $^{3}J_{HH} \approx {}^{1}J_{PH}$ = 7.2 Hz $PC\underline{H}(CH_3)_2$), 1.17 (72H, dd, $^{3}J_{HH} = 7.2$ Hz, $^{3}J_{PH} = 14.2$ Hz, $PCH(C\underline{H_3})_2$). $^{31}P\{^{1}H\}$-NMR (C_6D_6, 161.9 MHz) δ_P in ppm: 30.9 (s, br), 19.7 (s, br)

1.1.2 Complexes with Cu:M:S = 2:2:4

$[(^{i}Pr_3PCu)_2(GaMe_2)_2(SCH_2CH_2S)_2]$ (2)

In a Schlenk tube 0.65 g (0.60 mmol) of **1** are dissolved in 10 ml toluene and 1 ml THF. A greenish-yellow solution is obtained. 0.45 ml (2.40 mmol) of $GaMe_3 \cdot Et_2O$ are added while stirring the solution, which now turns yellow. 1.2 ml of a one molar solution of $HSCH_2CH_2SH$ (1.2 mmol) in toluene are added while stirring at ambient temperature. The solution initially evolves gas and is stirred for at least one hour at ambient temperature. The colour of the reaction mixture faints after several minutes and a colourless, clear solution is obtained. After layering with 10 ml of *n*-heptane the solution is kept over night at 2 °C and then one more day at -20 °C. During these days colourless crystals form while the *n*-heptane slowly diffused into the toluene solution. To assure complete crystallization the solution can be kept two more days at -20 °C. Now the cool solution is decanted from the colourless crystals and the crystalline product dried in vacuo. Yield: 0.75 g (78 %). ^{1}H-NMR (C_6D_6, 400 MHz) δ_H in ppm: 3.30 (4H, m, ethylene), 2.80 (4H, m, ethylene), 1.73 (6H, pseudo-octet, $^{3}J_{HH} \approx {}^{1}J_{PH}$ = 7.2 Hz $PC\underline{H}(CH_3)_2$), 1.03 (36H, dd, $^{3}J_{HH} = 7.2$ Hz, $^{3}J_{PH} = 14.2$ Hz, $PCH(C\underline{H_3})_2$), 0.35 (12H, s, Ga-$C\underline{H_3}$). $^{31}P\{^{1}H\}$-NMR (C_6D_6, 161.9 MHz) δ_P in ppm: 34.4. Elemental Analysis found (calculated for $C_{26}H_{62}P_2S_4Cu_2Ga_2$): C % = 37.59 (37.56); H % = 7.80 (7.52); S % = 15.35 (15.42). Following the experimental procedure for **2** the compounds **3**-**9** are obtained using the same molar ratio of starting materials.

Altering the molar ratio of starting materials to 3 equivalents of $[(^{i}Pr_3PCu)_4(SCH_2CH_2S)_2]$ (**1**), 4 equivalents of MR_3 (M = Ga, In; R = Me, Et, ^{i}Pr, ^{n}Bu) and 2 equivalents of $HSCH_2CH_2SH$ leads to compounds **10**-**17**.

[(^{i}Pr$_3$PCu)$_2$(GaEt$_2$)$_2$(SCH$_2$CH$_2$S)$_2$] (3)

Yield: 97 %. ^{1}H-NMR (C_6D_6, 400 MHz) δ_H in ppm: 3.32 (4H, m, ethylene), 2.82 (4H, m, ethylene), 1.74 (6H, pseudo-octet, $^3J_{HH} \approx {}^1J_{PH}$ = 7.2 Hz, PC$\underline{H}$(CH$_3$)$_2$), 1.63 (12H, t, $^3J_{HH}$ = 8.0 Hz, GaCH$_2$C$\underline{H_3}$), 1.03 (36H, dd, $^3J_{HH}$ = 7.2 Hz, $^3J_{PH}$ = 14.2 Hz, PCH(C$\underline{H_3}$)$_2$), 1.02 (8H, completely overlapped m, GaC$\underline{H_2}$CH$_3$). ^{31}P{^{1}H}-NMR (C_6D_6, 161.9 MHz) δ_P in ppm: 33.1. Elemental Analysis found (calculated): C % = 40.63 (40.60); H % = 8.21 (7.95); S % = 14.33 (14.45).

[(^{i}Pr$_3$PCu)$_2$(Ga^{i}Pr$_2$)$_2$(SCH$_2$CH$_2$S)$_2$] (4)

Yield: 91 %. ^{1}H-NMR (C_6D_6, 400 MHz) δ_H in ppm: 3.33 (4H, m, ethylene), 2.88 (4H, m, ethylene), 1.76 (6H, overlapped pseudo-octet, $^3J_{HH} \approx {}^1J_{PH}$ = 7.2 Hz PC$\underline{H}$(CH$_3$)$_2$), 1.73 (12H, overlapped d, $^3J_{HH}$ = 7.4 Hz, GaCH$_2$(C$\underline{H_3}$)$_2$), 1.68 (12H, d, $^3J_{HH}$ = 7.4 Hz, GaCH$_2$(C$\underline{H_3}$)$_2$), 1.31 (4H, septet, $^3J_{HH}$ = 7.4 Hz, Ga$\underline{CH_2}$(CH$_3$)$_2$), 1.03 (36H, dd, $^3J_{HH}$ = 7.2 Hz, $^3J_{PH}$ = 14.2 Hz, PCH(C$\underline{H_3}$)$_2$). ^{31}P{^{1}H}-NMR (C_6D_6, 161.9 MHz) δ_P in ppm: 32.6. Elemental Analysis found (calculated): C % = 43.29 (43.27); H % = 8.58 (8.33); S % = 13.23 (13.59).

[(^{i}Pr$_3$PCu)$_2$(Ga^{n}Bu$_2$)$_2$(SCH$_2$CH$_2$S)$_2$] (5)

Yield: 50 %. ^{1}H-NMR (C_6D_6, 400 MHz) δ_H in ppm: 3.34 (4H, m, SC$_2$H$_4$S), 2.83(4H, m, SC$_2$H$_4$S), 1.95 (8H, m, GaCH$_2$C$\underline{H_2}$C$_2$H$_5$), 1.73 (6H, pseudo-octet, $^3J_{HH} \approx {}^1J_{PH}$ = 7.2 Hz PC$\underline{H}$(CH$_3$)$_2$), 1.64 (8H, sextet, GaC$_2$H$_4$C$\underline{H_2}$CH$_3$, $^3J_{HH}$ = 7.3 Hz), 1.09 (12H, t overlapped, $^3J_{HH}$ = 7.3 Hz, GaC$_3$H$_6$C$\underline{H_3}$), 1.08 (36H, dd, $^3J_{HH}$ = 7.2 Hz, $^3J_{PH}$ = 14.2 Hz, PCH(C$\underline{H_3}$)$_2$), 1.0 (4H, t, $^3J_{HH}$ = 8.3 Hz, GaC$\underline{H_2}$C$_3$H$_7$). ^{31}P{^{1}H}-NMR (C_6D_6, 161.9 MHz) δ_P in ppm: 34.1. Elemental Analysis found (calculated): C % = 45.63 (45.65); H % = 8.59 (8.67); S % = 12.50 (12.83).

[(^{i}Pr$_3$PCu)$_2$(InMe$_2$)$_2$(SCH$_2$CH$_2$S)$_2$] (6)

Yield: 82 %. ^{1}H-NMR (C_6D_6, 400 MHz) δ_H in ppm: 3.28 (4H, m, ethylene), 2.89(4H, m, ethylene), 1.73 (6H, pseudo-octet, $^3J_{HH} \approx {}^1J_{PH}$ = 7.2 Hz PC$\underline{H}$(CH$_3$)$_2$), 1.03 (36H, dd, $^3J_{HH}$ = 7.2 Hz, $^3J_{PH}$ = 14.2 Hz, PCH(C$\underline{H_3}$)$_2$), 0.29 (6H, s, InC$\underline{H_3}$), ^{31}P{^{1}H}-NMR (C_6D_6, 161.9 MHz) δ_P in ppm: 34.3. Elemental Analysis found (calculated): C % = 33.88 (33.88); H % = 6.81 (6.78); S % = 13.74 (13.91).

[(^{i}Pr$_3$PCu)$_2$(InEt$_2$)$_2$(SCH$_2$CH$_2$S)$_2$] (7)

Yield: 88 %. ^{1}H-NMR (C_6D_6, 400 MHz) δ_H in ppm: 3.25 (4H, br m, ethylene), 2.87 (4H, br m, ethylene), 1.71 (6H, overlapped pseudo-octet, $^3J_{HH} \approx {}^1J_{PH}$ = 7.2 Hz, PC$\underline{H}$(CH$_3$)$_2$), 1.66 (12H, overlapped t, $^3J_{HH}$ = 8.0 Hz, InCH$_2$C$\underline{H_3}$), 1.07 (8H, overlapped q, $^3J_{HH}$ = 8.0 Hz, InC$\underline{H_2}$CH$_3$), 1.03 (36H, overlapped dd, $^3J_{HH}$ = 7.1 Hz, $^3J_{PH}$ = 14.2 Hz, PCH(C$\underline{H_3}$)$_2$). ^{31}P{^{1}H}-NMR (C_6D_6, 161.9 MHz) δ_P in ppm: 34.2. Elemental Analysis found (calculated): C % = 36.86 (36.85); H % = 7.39 (7.22); S % = 12.76 (13.12).

[(^{i}Pr$_3$PCu)$_2$(In^{i}Pr$_2$)$_2$(SCH$_2$CH$_2$S)$_2$] (8)

Yield: 85 %. ^{1}H-NMR (C_6D_6, 400 MHz) δ_H in ppm: 3.30 (4H, m, ethylene), 2.93 (4H, m, ethylene), 1.81 (12H, overlapped d, $^3J_{HH}$ = 7.6 Hz, InCH$_2$(C$\underline{H_3}$)$_2$), 1.78 (6H, completely overlapped, PC$\underline{H}$(CH$_3$)$_2$), 1.76 (12H, overlapped d, $^3J_{HH}$ = 7.6 Hz, InCH$_2$(C$\underline{H_3}$)$_2$), 1.31 (4H, septet, $^3J_{HH}$ = 7.6 Hz, In$\underline{CH_2}$(CH$_3$)$_2$), 1.06 (36H, dd, $^3J_{HH}$ = 7.2 Hz, $^3J_{PH}$ = 14.2 Hz, PCH(C$\underline{H_3}$)$_2$). ^{31}P{^{1}H}-NMR (C_6D_6, 161.9 MHz) δ_P in ppm: 35.1. Elemental Analysis found (calculated): C % = 39.34 (39.50); H % = 7.81 (7.60); S % = 12.05 (12.40).

[(^{i}Pr$_3$PCu)$_2$(In^{n}Bu$_2$)$_2$(SCH$_2$CH$_2$S)$_2$] (9)

Yield: 50 %. ^{1}H-NMR (C_6D_6, 400 MHz) δ_H in ppm: 3.32 (4H, m, SC$_2$H$_4$S), 2.93(4H, m, SC$_2$H$_4$S), 2.04 (8H, quintet, InCH$_2$C$\underline{H_2}$C$_2$H$_5$, $^3J_{HH}$ = 7.3 Hz), 1.81 (6H, pseudo-octet, $^3J_{HH} \approx {}^1J_{PH}$ = 7.1 Hz PC$\underline{H}$(CH$_3$)$_2$), 1.64 (8H, sextet, InC$_2$H$_4$C$\underline{H_2}$CH$_3$, $^3J_{HH}$ = 7.3 Hz), 1.18 (4H, dt, $^3J_{HH}$ = 8.3 Hz, $^3J_{HH}$ = 3.3 Hz, InC$\underline{H_2}$C$_3$H$_7$, 1.09 (36H, dd, $^3J_{HH}$ = 7.2 Hz, $^3J_{PH}$ = 14.2 Hz, PCH(C$\underline{H_3}$)$_2$), 1.08 (12H, t overlapped, InC$_3$H$_6$C$\underline{H_3}$). ^{31}P{^{1}H}-NMR (C_6D_6, 161.9 MHz) δ_P in ppm: 35.1. Elemental Analysis found (calculated): C % = 42.08 (41.87); H % = 7.95 (8.08); S % = 11.76 (12.08).

1.1.3 Complexes with Cu:M:S = 3:1:4

[(^{i}Pr$_3$PCu)$_3$(GaMe$_2$)(SCH$_2$CH$_2$S)$_2$] (10)

Yield: 75 %. ^{1}H-NMR (C_6D_6, 400 MHz) δ_H in ppm: 3.35 (2H, m, ethylene), 3.11 (4H, m, ethylene), 2.77 (2H, m, ethylene), 1.76 (9H, m, PC$\underline{H}$(CH$_3$)$_2$), 1.08 (54H, m, PCH(C$\underline{H_3}$)$_2$), 0.42 and 0.35 (6H, s, GaC$\underline{H_3}$). ^{31}P{^{1}H}-NMR (C_6D_6, 161.9 MHz) δ_P in ppm: 34.4, 33.7, 20.0 (br). Elemental Analysis found (calculated): C % = 41.47 (41.48); H % = 8.31 (8.12); S % = 12.92 (13.42).

[(^{i}Pr$_3$PCu)$_3$(GaEt$_2$)(SCH$_2$CH$_2$S)$_2$] (11)

Yield: 58 %. ^{1}H-NMR (C_6D_6, 400 MHz) δ_H in ppm: 3.35 (2H, m, ethylene), 3.11 (4H, m, br, ethylene), 2.77 (2H, m, ethylene), 1.78 (8H, m, br, PC$\underline{H}$(CH$_3$)$_2$), 1.70 and 1.63 (6H, t, $^{3}J_{HH}$ = 8.0 Hz, GaCH$_2$C$\underline{H_3}$), 1.08 (58H, overlapped m, br, PCH(C$\underline{H_3}$)$_2$ and GaC$\underline{H_2}$CH$_3$). ^{31}P{^{1}H}-NMR (C_6D_6, 161.9 MHz) δ_P in ppm: 34.3, 33.6, 19.6 (br). Elemental Analysis found (calculated): C % = 42.74 (42.74); H % = 8.06 (8.30); S % = 11.74 (13.04).

[(^{i}Pr$_3$PCu)$_3$(Ga^{i}Pr$_2$)(SCH$_2$CH$_2$S)$_2$] (12)

Yield: 79 %. ^{1}H-NMR (C_6D_6, 400 MHz) δ_H in ppm: 3.33 (2H, m, ethylene), 3.10 (4H, m, br, ethylene), 2.83 and 2.67 (2H, m, ethylene), 1.78 (21H, m, br, overlapped, PC$\underline{H}$(CH$_3$)$_2$ and GaCH(C$\underline{H_3}$)$_2$), 1.40 (2H, septet, $^{3}J_{HH}$= 7.5 Hz, GaC$\underline{H}$(CH$_3$)$_2$) 1.09 (54H, overlapped m, br, PCH(C$\underline{H_3}$)$_2$). ^{31}P{^{1}H}-NMR (C_6D_6, 161.9 MHz) δ_P in ppm: 32.4, 18.4 (br). Elemental Analysis found (calculated): C % = 43.82 (43.93); H % = 8.20 (8.47); S % = 12.08(12.68).

[(^{i}Pr$_3$PCu)$_3$(Ga^{n}Bu$_2$)(SCH$_2$CH$_2$S)$_2$] (13)

Yield: 71 %. ^{1}H-NMR (C_6D_6, 300 MHz) δ_H in ppm: 3.40 - 2.50 (8H, m, br, SC$_2$H$_4$S), 1.98 (4H, m, GaCH$_2$C$\underline{H_2}$C$_2$H$_5$) 1.74 (13H, m, overlapped, PC$\underline{H}$(CH$_3$)$_2$ and GaC$_2$H$_4$C$\underline{H_2}$CH$_3$), 1.09 (64H, overlapped m, br, PCH(C$\underline{H_3}$)$_2$, GaC$_3$H$_6$C$\underline{H_3}$, GaC$\underline{H_2}$C$_3$H$_7$), ^{31}P{^{1}H}-NMR (C_6D_6, 161.9 MHz) δ_P in ppm: 34.2, 33.7 20.0 (br). Elemental Analysis found (calculated): C % = 45.08 (45.06); H % = 8.56 (8.63); S % = 11.85 (12.33).

[(^{i}Pr$_3$PCu)$_3$(InMe$_2$)(SCH$_2$CH$_2$S)$_2$] (14)

Yield: 71 %. ^{1}H-NMR (C_6D_6, 400 MHz) δ_H in ppm: 3.35 (8H, m, br, ethylene), 1.80 (9H, m, PC$\underline{H}$(CH$_3$)$_2$), 1.14 (54H, m, PCH(C$\underline{H_3}$)$_2$), 0.34 and 0.29 (6H, s, InC$\underline{H_3}$). ^{31}P{^{1}H}-NMR (C_6D_6, 161.9 MHz) δ_P in ppm: 34.0, 32.8, 18.5 (br). Elemental Analysis found (calculated): C % = 39.59 (39.61); H % = 7.79 (7.76); S % = 12.51 (12.82).

[(^{i}Pr$_3$PCu)$_3$(InEt$_2$)(SCH$_2$CH$_2$S)$_2$] (15)

Yield: 88 %. ^{1}H-NMR (C_6D_6, 400 MHz) δ_H in ppm: 3.08 (8H, m, br, ethylene), 1.78 (8H, overlapped m, br, PC$\underline{H}$(CH$_3$)$_2$), 1.75 and 1.71 (6H, overlapped t, $^{3}J_{HH}$ = 8.0 Hz, InCH$_2$C$\underline{H_3}$), 1.10 (58H, overlapped m, br, PCH(C$\underline{H_3}$)$_2$ and InC$\underline{H_2}$CH$_3$). ^{31}P{^{1}H}-NMR (C_6D_6, 161.9 MHz) δ_P in ppm: 34.3, 32.9, 18.9 (br). Elemental Analysis found (calculated): C % = 40.88 (40.87); H % = 7.72 (7.94); S % = 12.46 (12.47).

[(^{i}Pr$_3$PCu)$_3$(In^{i}Pr$_2$)(SCH$_2$CH$_2$S)$_2$] (16)

Yield: 92 %. ^{1}H-NMR (C_6D_6, 400 MHz) δ_H in ppm: 3.36 - 2.60 (8H, m, br, ethylene), 1.80 (21H, m, br, overlapped, PC$\underline{H}$(CH$_3$)$_2$ and GaCH(C$\underline{H_3}$)$_2$), 1.62 (2H, septet, $^{3}J_{HH}$= 7.5 Hz, GaC$\underline{H}$(CH$_3$)$_2$), 1.10 (54H, overlapped m, br, PCH(C$\underline{H_3}$)$_2$). ^{31}P{^{1}H}-NMR (C_6D_6, 161.9 MHz) δ_P in ppm: 32.4 and 18.4 (br). Elemental Analysis found (calculated): C % = 41.82 (42.06); H % = 7.76 (8.11); S % = 12.89 (12.14).

[($^{i}Pr_3PCu)_3(In^{n}Bu_2)(SCH_2CH_2S)_2$] (17)

Yield: 54 %. ^{1}H-NMR (C_6D_6, 400 MHz) δ_H in ppm: 3.38 - 2.60 (8H, m, br, SC_2H_4S), 2.04 (4H, quintet, $InCH_2C\underline{H_2}C_2H_5$, $^{3}J_{HH}$ = 7.3 Hz), 1.81 (9H, pseudo-octet, $^{3}J_{HH} \approx {}^{1}J_{PH}$ = 7.1 Hz $PC\underline{H}(CH_3)_2$), 1.64 (4H, sextet, $InC_2H_4C\underline{H_2}CH_3$, $^{3}J_{HH} = 7.3$ Hz), 1.18 (4H, dt, br, $^{3}J_{HH} = 7.8$ Hz, $InC\underline{H_2}C_3H_7$, 1.11 (36H, m, overlapped, $PCH(C\underline{H_3})_2$, $InC_3H_6C\underline{H_3}$). $^{31}P\{^{1}H\}$-NMR (C_6D_6, 161.9 MHz) δ_P in ppm: 35.2, 34.2 and 20.2 (br). Elemental Analysis found (calculated): C % = 43.24 (43.18); H % = 8.15 (8.27); S % = 11.79 (11.82).

1.2 X-ray single crystal structure analysis

Crystal structures were determinded by measurements with an area detector system from STOE (IPDS 1 or IPDS-2T). The single crystals were covered with mineral oil and mounted on a thin glass fiber attached to the goniometer head. The prepared single crystal samples were cooled down to 213 K (IPDS 1) or 180 K or 100 K (IPDS-2T) before measurement, thus freezing the mineral oil and fixing the crystal. Source of radiation was a sealed X-ray tube with a Mo-anode (λ (Mo-K$_\alpha$) = 71,073 pm, 50 kV, 40 mA) driven with a graphite monochromator. The data collection, unit cell determination, integration and absorption correction were handeled using the Program X-Area[1]. The crystal structures were solved by direct methods using the interface program WINGX[2] including the programs SHELXS-97[3] and SIR-92[4] for crystal structure determination. Refinement was performed with the program SHELXL-97[3]. Figures of structures were created using the program DIAMOND 3[5]. Files (.cif, .fcf, .hkl) of single crystal structures presented in this publication are deposited in the *Cambridge Structural Database*.

Compound	CCDC No.	Comments on checkcif alerts
3	907031	
4	907032	
6	907033	
7	907034	
8	907035	
9	907036	level A and B: completeness lower than 93 % caused by triclinic symmetry and data collection using STOE IPDS 1 (only incremental rotation about φ)
10	907023	
11	907024	
12	907025	
13	907026	
14	907027	
15	907028	
16	907029	
17	907030	

Tab. S 1 Overview of CCDC numbers and comments on checkcif alerts in presented structures

Inversion symmetry can be found in the complex molecules of **2**, **4**, **7**, **8** and **9**, while inversion centres are in between the tetranuclear molecules in **6**. The coordination sphere of the copper atom is almost trigonal planar. The out of plane distance ranges between 13 and 25 pm. The Cu-S distances range between 225 and 230 pm. Due to the different atomic radii, the Ga-S distances measure between 234 and 238 pm and are 20 pm shorter than the In-S bonds (255 - 258 pm). Thus, no noteworthy change in the mentioned eight-membered ring formed by copper, sulphur and the group(III) metal atoms occurs within the obtained complexes.

The difference between the homologous MMe_2 compounds **2** (M = Ga, C 2/c) and **6** (M = In, P 2$_1$/c) originate from different molecule packing. Within the MEt_2 compounds **3** and **7** crystallize with very similar lattice parameters, however, the structure of the gallium complex **3** can only be refined in the non-centrosymmetric space group P 2$_1$ while **7** is centrosymmetric (P 2$_1$/n). By transforming the atomic coordinates in **3** according to the standard setting[6] for P 2$_1$/n, the coordinates of Ga2 and Cu2 are too far away from a possible symmetry equivalent position to Ga1 and Cu1 for a refinement in the centrosymmetric group. The structures of the $M^{i}Pr_2$ compounds are close to being isostructural, except for an eclipsed arrangement for the ^{i}Pr groups of the $Ga^{i}Pr_2$ units in **4** and a staggered one for the $In^{i}Pr_2$ units in **8**. A triclinic form of the $In^{n}Bu_2$ compound **9** could be crystallized

and its structure solved and refined in P $\bar{1}$. However, problems occurred during refinement of the structure of **5**. The diffraction pattern suggested a monoclinic cell for which the heavy atoms of this structure could be well resolved. However, the arrangement of *n*-butyl groups within the molecules in **5** could not be resolved. Along each cell axis superstructural reflections were observed, which would cause at least doubling of each cell axis. Based on these observations it was attempted to describe differently arranged *n*-butyl groups by superstructural models. But despite several recrystallizations of **5**, no data sets could be collected that would allow for an acceptable solution of this superstructure. Whereas a similar cell and the same superstructural effects could be observed, but not resolved for a recrystallized batch of **9**, a triclinic form of **5** could not be obtained. Nevertheless, the connectivity of atoms within the molecular structure of **5** could be proven to be analogous to **2**-**4** and **6**-**9**.

By formal replacement of one R_2M^{III} unit by CuP^iPr_3, the molecular structures of $[(^iPr_3PCu)_3(MR_2)(SCH_2CH_2S)_2]$ (**10**-**17**) can be derived from the ones of $[(^iPr_3PCu)_2(MR_2)_2(SCH_2CH_2S)_2]$ (**2**-**9**). By this replacement a non-chelated CuP^iPr_3 is obtained, which bonds to one sulphur atom of each of the two 1,2-ethanedithiolates. The out of plane distance of the copper(I) atom in the non-chelated unit is, with only 1 - 6 pm, smaller than in the chelated units (10 - 20 pm). Apart from that, in the molecular structures of **10**-**17** no significant changes in bond distances can be observed for the remaining groups, when compared to the molecular structures of **2**-**9**. Within the complexes **10**-**13**, the two M^nBu_2 compounds **13** and **17** are isomorphous, considering a maximal difference of 15 pm for the *b*-axes in both unit cells. These are the only two exhibiting a higher symmetry than triclinic. The other complexes exhibit a more or less obvious isostructural relation towards each other. The $GaEt_2$ compound **11** and the M^iPr_2 compounds **12** and **16** crystallize with nearly the same cell parameters. The unit cells of the MMe_2 compounds **10** and **14** can be transformed into the same arrangements by using the following transformation matrix.

$$\begin{pmatrix} 0 & 1 & 0 \\ -1 & 0 & 0 \\ 0 & 0 & 1 \end{pmatrix}$$

However, this neglects the convention, $a < b < c$, for triclinic cells. The unit cell of the $InEt_2$ compound **15** is twice the size of the other triclinic cells. This arises from two different alternating arrangements of $InEt_2$ groups within the different molecules, which causes the structure of **15** to be a superstructure of the cell of the $GaEt_2$ compound **11**. The cell of **11** can be transformed into a similar cell as for **15** by using the following transformation matrix.

$$\begin{pmatrix} 0 & -1 & 0 \\ -1 & 0 & 1 \\ -1 & 1 & -1 \end{pmatrix}$$

Hence, the compounds **10**-**12** and **14**-**16** exhibit almost exactly the same packing of molecules.

1.3 Simultaneous thermal analysis

Simultaneous thermal analysis was performed using a "STA 449 F1 Jupiter" TG/DTA device (Netzsch) coupled with a "Tensor 27" FTIR spectrometer (Bruker) and a "QMS 403 C" electron ionization quadrupole mass spectrometer (Aëolos). The samples were transfered into Al_2O_3 crucibles within a drybox under nitrogen atmosphere. The samples were then transported to the STA device in a dry vessel in order to minimize contact with air. The oven was evacuated and flooded with helium carrier gas before measurements were started. The samples were heated from 10-600 °C with a rate of 10 K/min. DTA reference was an empty Al_2O_3 crucible.

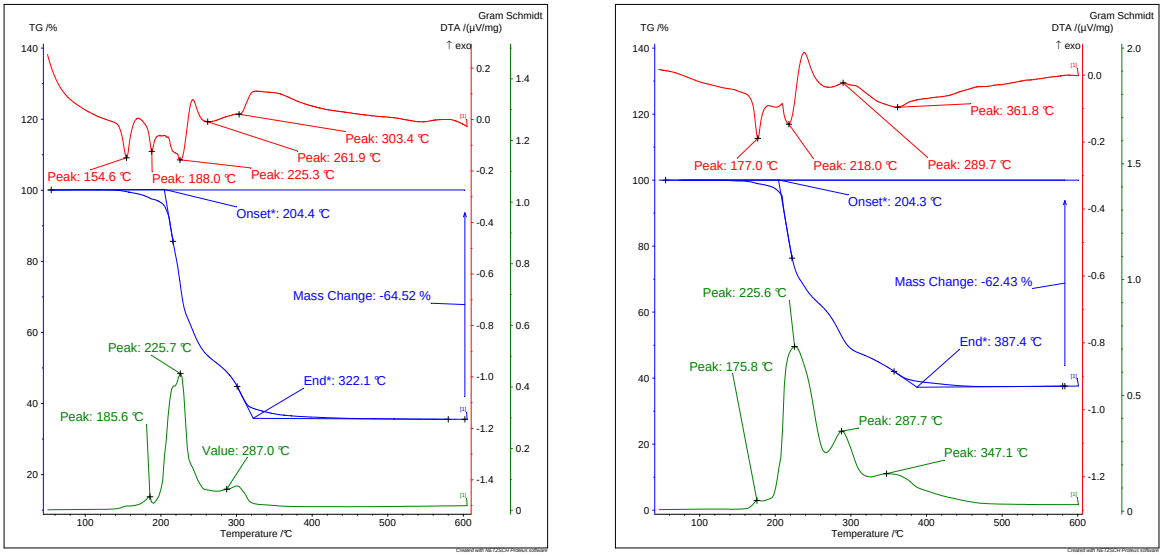

Fig. S 1 left: $[(^iPr_3PCu)_2(GaMe_2)(SCH_2CH_2S)_2]$ (**2**); right: $[(^iPr_3PCu)_2(GaEt_2)(SCH_2CH_2S)_2]$ (**3**).

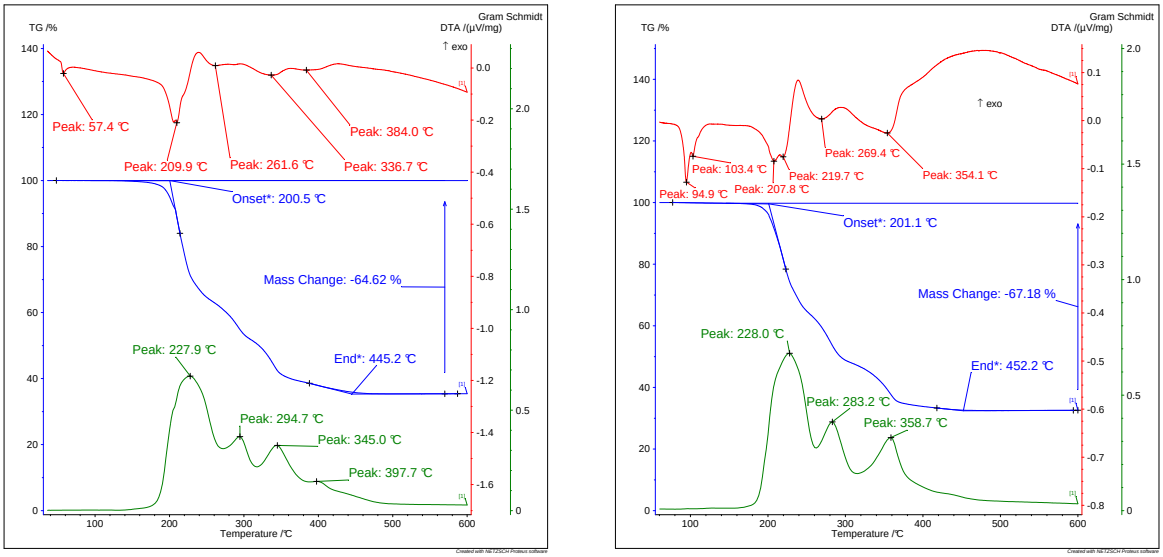

Fig. S 2 left: $[(^{i}Pr_3PCu)_2(Ga^{i}Pr_2)(SCH_2CH_2S)_2]$ (**4**); right: $[(^{i}Pr_3PCu)_2(Ga^{n}Bu_2)(SCH_2CH_2S)_2]$ (**5**).

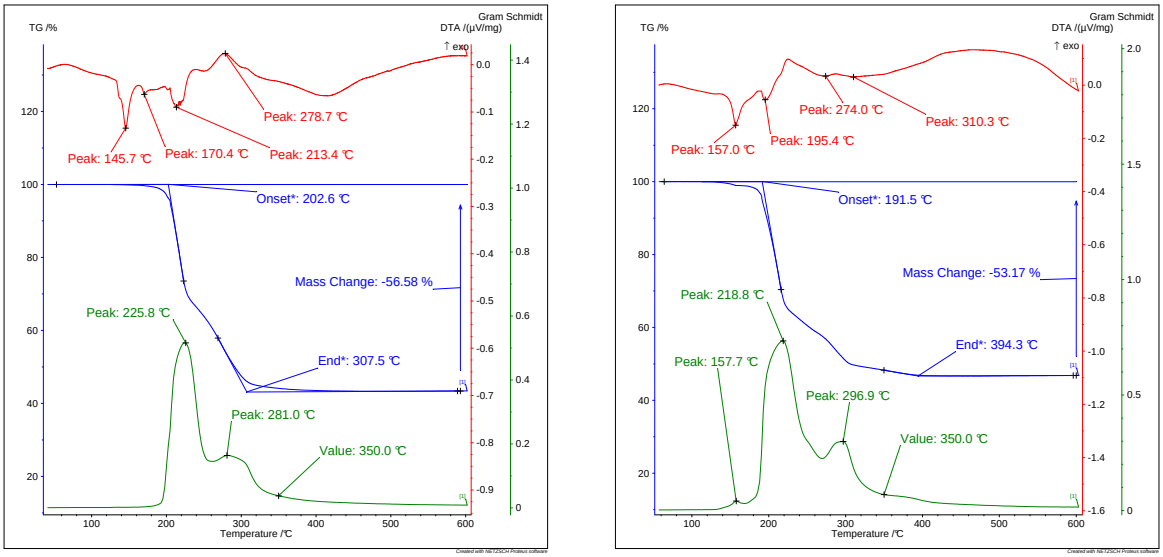

Fig. S 3 left: $[(^{i}Pr_3PCu)_2(InMe_2)(SCH_2CH_2S)_2]$ (**6**); right: $[(^{i}Pr_3PCu)_2(InEt_2)(SCH_2CH_2S)_2]$ (**7**).

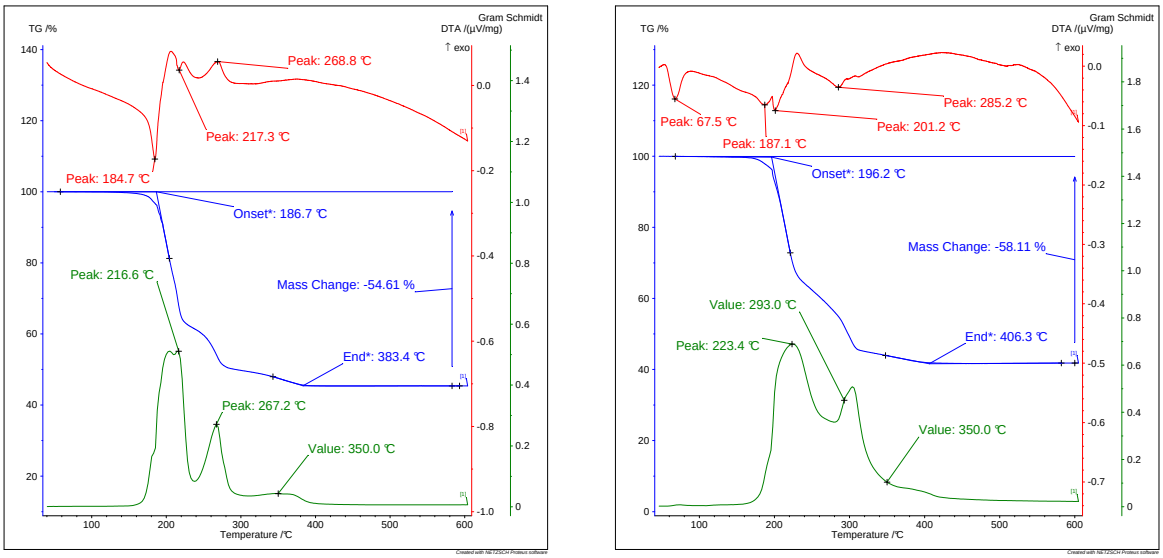

Fig. S 4 left: $[(^{i}Pr_3PCu)_2(In^{i}Pr_2)(SCH_2CH_2S)_2]$ (**8**); right: $[(^{i}Pr_3PCu)_2(In^{n}Bu_2)(SCH_2CH_2S)_2]$ (**9**).

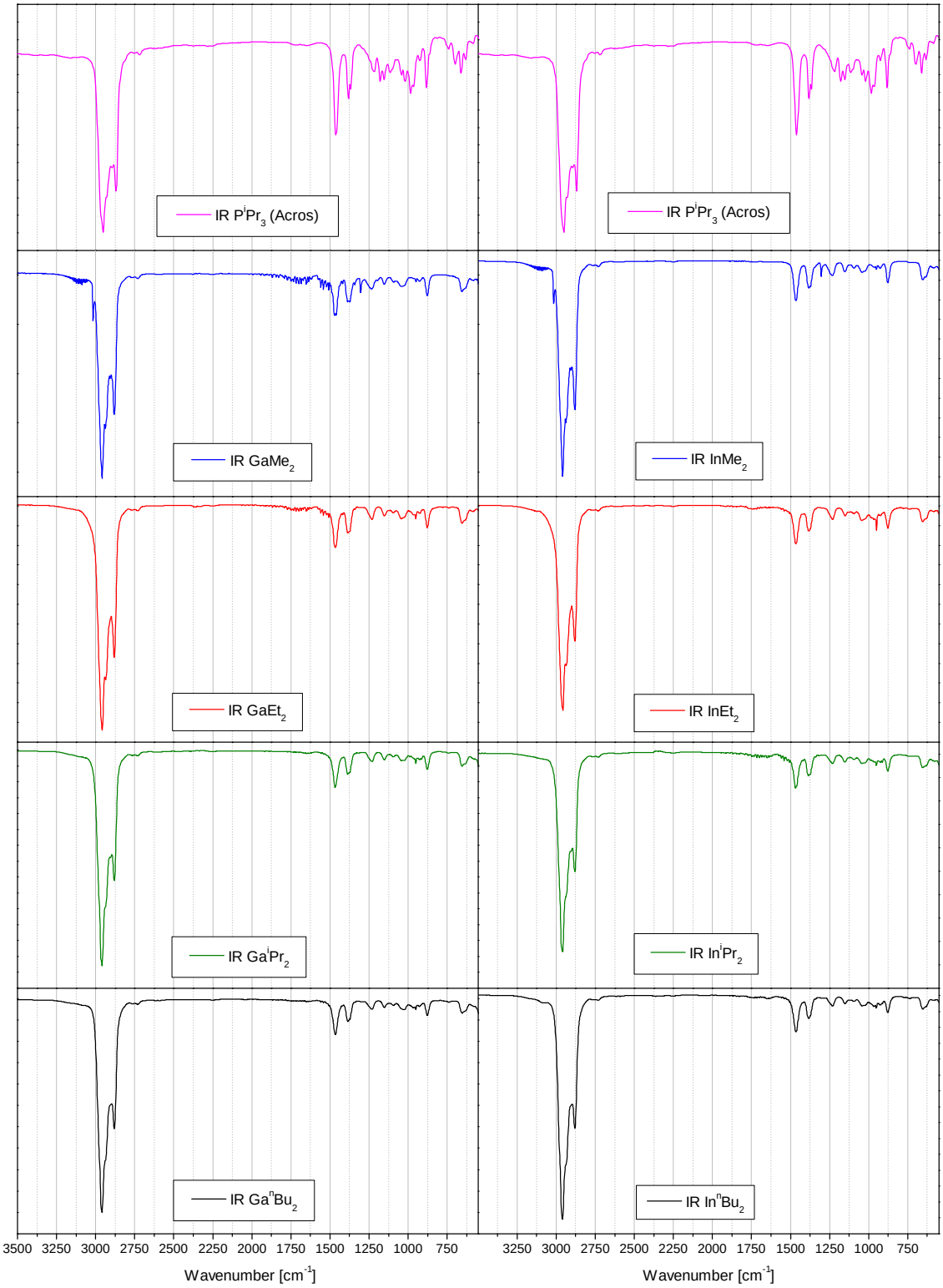

Fig. S 5 Gas phase IR-spectra of the volatile thermolysis products of [(^{i}Pr$_3$PCu)$_2$(MR$_2$)$_2$(SCH$_2$CH$_2$S)$_2$] (MR$_2$ = GaMe$_2$ (**2**), GaEt$_2$ (**3**), Ga^{i}Pr$_2$ (**4**), Ga^{n}Bu$_2$ (**5**) and InMe$_2$ (**6**), InEt$_2$ (**7**), In^{i}Pr$_2$ (**8**), In^{n}Bu$_2$ (**9**)) at 220(±5) °C during STA in comparison with reference IR spectrum of P^{i}Pr$_3$.

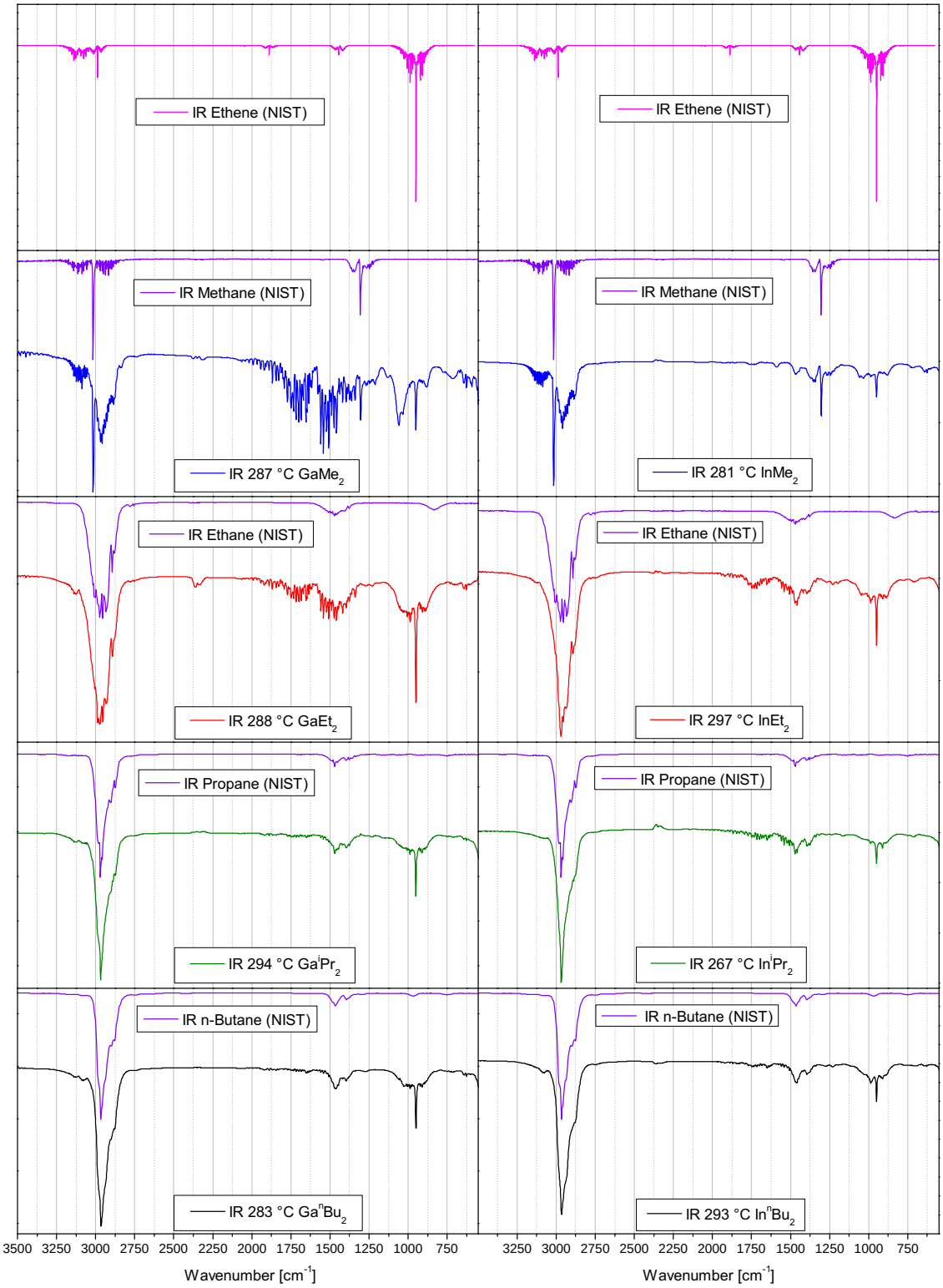

Fig. S 6 Gas phase IR-spectra of the volatile thermolysis products of $[(^{i}Pr_3PCu)_2(MR_2)_2(SCH_2CH_2S)_2]$ (MR_2 = $GaMe_2$ (**2**), $GaEt_2$ (**3**), $Ga^{i}Pr_2$ (**4**), $Ga^{n}Bu_2$ (**5**) and $InMe_2$ (**6**), $InEt_2$ (**7**), $In^{i}Pr_2$ (**8**), $In^{n}Bu_2$ (**9**)) recorded around 290 °C during STA in comparison with reference IR-spectra of methane and ethene.

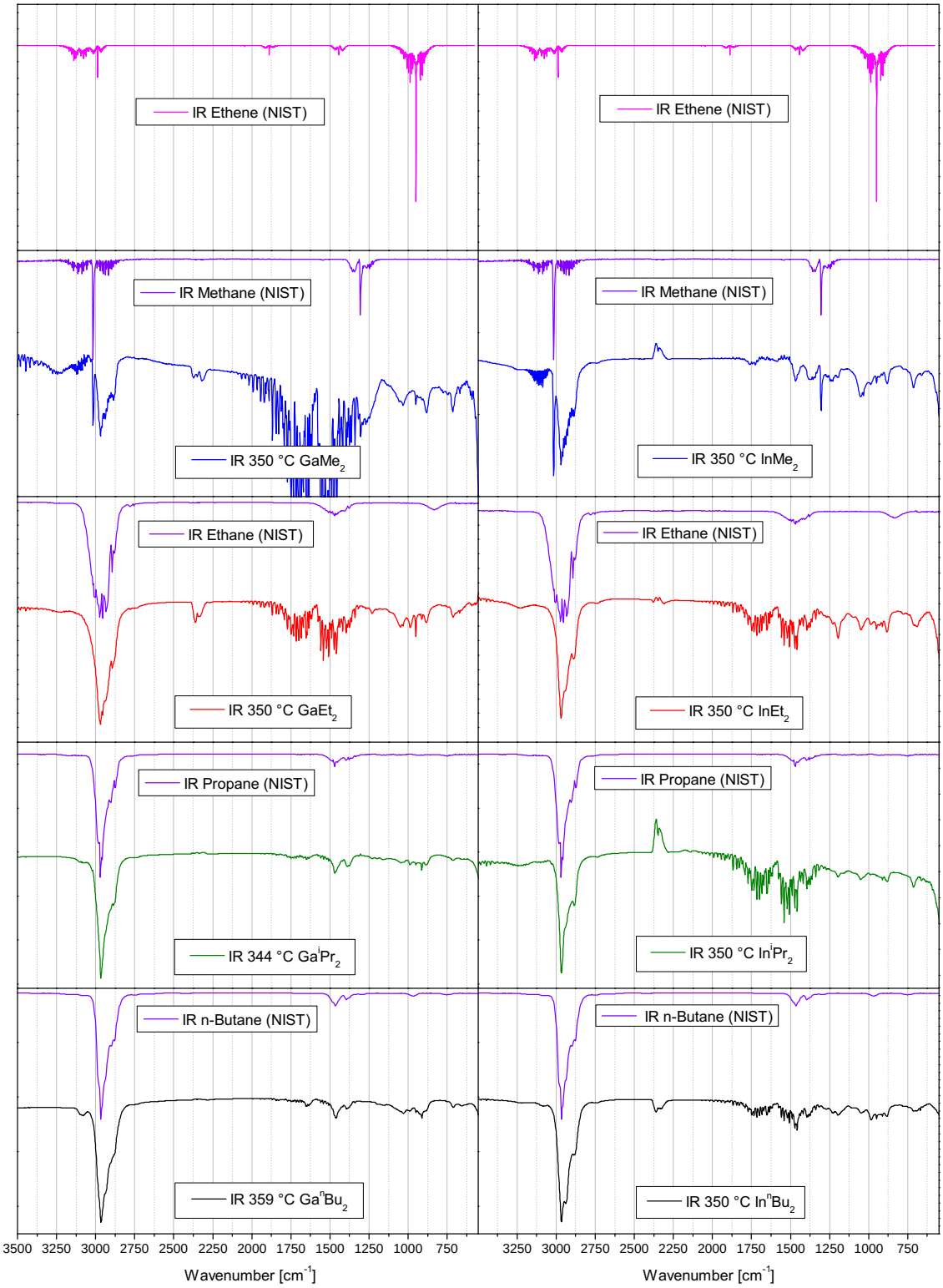

Fig. S 7 Gas phase IR-spectra of the volatile thermolysis products of $[(^{i}Pr_3PCu)_2(MR_2)_2(SCH_2CH_2S)_2]$ (MR_2 = $GaMe_2$ (**2**), $GaEt_2$ (**3**), $Ga^{i}Pr_2$ (**4**), $Ga^{n}Bu_2$ (**5**) and $InMe_2$ (**6**), $InEt_2$ (**7**), $In^{i}Pr_2$ (**8**), $In^{n}Bu_2$ (**9**)) recorded around 350 °C during STA in comparison with reference IR-spectra of methane and ethene.

1.4 X-ray powder diffractometry and Rietveld phase analysis

Powder X-ray diffraction data were collected using a STOE STADIP powder diffractometer with Debye-Scherre geometry. Source of radiation was a sealed tube with Cu-anode (λ (Cu-$K_{\alpha 1}$) = 154.06 pm). The radiation was monochromatized using a Ge-single crystal in [111]-orientation. All measurements were performed in transmission mode at room temperature using a position sensitive detector. Residues that did not contain indium were sealed in a glass capillary with an inner diameter of 0.3 mm. The measurements were performed under continous ϕ-rotation. Samples containing indium were measured in transmission mode with a flat sample geometry. The powdered samples were spread evenly on a circular polymer with diluted glue (”Elmer’s white glue”). When the samples had been dried, they were covered with a second piece of film, inserted into a sample holders and fixed with a mask of 1 cm inner diameter. These samples were measured in an 2θ-ω-coupled mode and continuously rotating around the sample center on an axis perpendicular to the sample surface. The program WIN XPOW[7] was used for data collection and data processing. Phase analysis of powder diffraction data was performed using the Rietveld method[8]. The program used for that purpose was GSAS[9] with the graphical interphase EXPGUI[10]. Functions used were: background function number 1 and profile function number 3.

The presented powder data refers to thermolysis residues that were obtained by heating the respective precursor compounds **2**-**9** in quartz tubes under a dry nitrogen atmosphere at 650 °C. Crystalline phases used for the refinements were chalcopyrite type $CuMS_2$ (M = Ga[11], In[12]), wurtzite type $CuMS_2$ (M = Ga[13], In[14]), digenite $Cu_{1.8}S$[15] or chalcocite Cu_2S[16,17], In_2O_3[18] and $Cu_{11}In_9$[19].

In a cooperation with the Max-Planck-Institute for Chemical Physics of Solids(Nöthnitzer Strae 40, 01187 Dresden Germany; by Dr. J. Hunger) samples of these thermolysis residues were investigated for by metal content analysis. For that purpose the residues were dissolved by microwave assisted digestion in HNO_3/HCl and the metal content of these solution was determined by inductive coupled plasma optical emission spectroscopy

In case of $CuInS_2$ containing residues the missing of several reflections of lower intensity was observed for refinement in the chalcopyrite type. Especially noticeable, the (1 0 1) reflection (17.9°for $Cu_{K\alpha 1}$) of the CP-$CuInS_2$ was either missing or had a very low intensity. As the isotropic displacement parameters were tried to be included into the refinement, the ones for the metal atoms refined to illogical values. The U_{iso} of indium became far to large, whereas the one for copper even refined to negative values. Such problems did not occur when refining the powder diffractograms of the $CuGaS_2$ containing residues. The problem in case of the $CuInS_2$ residues could be solved by altering the occupation between copper and indium. For this purpose the original CP-$CuInS_2$ with copper in (0, 0, 0) and indium in (0, 0, $\frac{1}{2}$) was changed into a disordered chalcopyrite-type model (dCP-type). In this dCP-type, the metal atoms are partially occupying the original CP-type positions and partially their inverse positions, hence, with copper in (0, 0, $\frac{1}{2}$) and indium (0, 0, 0). An occupation between 75:25 and 50:50 (original:inverse) was applied. These values had been found by changing the occupation from 100:0 to 50:50 and observing the development of the metal atom U_{iso} values. The occupation resulting in the most reasonable U_{iso} ($U_{iso}(Cu) > U_{iso}(In)$, $0.02 \leq U_{iso}(Cu) \leq 0.04$, $0.01 \leq U_{iso}(In) \leq 0.03$) was then chosen for the refinement. A complete disordered model of the CP-$CuInS_2$ should actually be describable by a zincblende-type $CuInS_2$ (ZB-type), meaning that only half of the tetragonal unit cell of CP-$CuInS_2$ with a 50:50 disorder of copper and indium in the metal atom sites is taken into account. This changes the space group from I $\bar{4}$2d for the tetragonal CP-$CuInS_2$ into F $\bar{4}$3m for the cubic ZB-$CuInS_2$. A Rietveld refinement in this space group has the same effect of having several reflections disappear due to additional symmetry. However, when applying this model to the collected PXRD data sets, several reflections that showed shoulders could not be properly refined. These observed shoulders arise from reflections that split up into pairs of reflections in I $\bar{4}$2d, whereas there are only single reflections in these positions in F $\bar{4}$3m. Fig. S 8 visualizes this observation. In this depiction, PXRD data of the thermolysis residue of $[(^iPr_3PCu)(InMe)_2(SC_2H_4S)_2]$ (**6**) was refined with the dCP and the ZB-type models. To see if ordering into CP-$CuInS_2$ can be achieved, a thermolysis residue of the same compound was heated to 950 °C and after cooling down to room temperature a powder data set was collected. The result can be seen in the top of Fig. S 8. In this case refinement using the CP-model delivered reasonable U_{iso} for copper and indium. It can be seen that several reflections appear, that cannot be detected in case of the 650 °C thermolysis residue. The coexistence of CP-$CuInS_2$ with other polymorphs derived from this structure have been predicted[20] and proven[21].

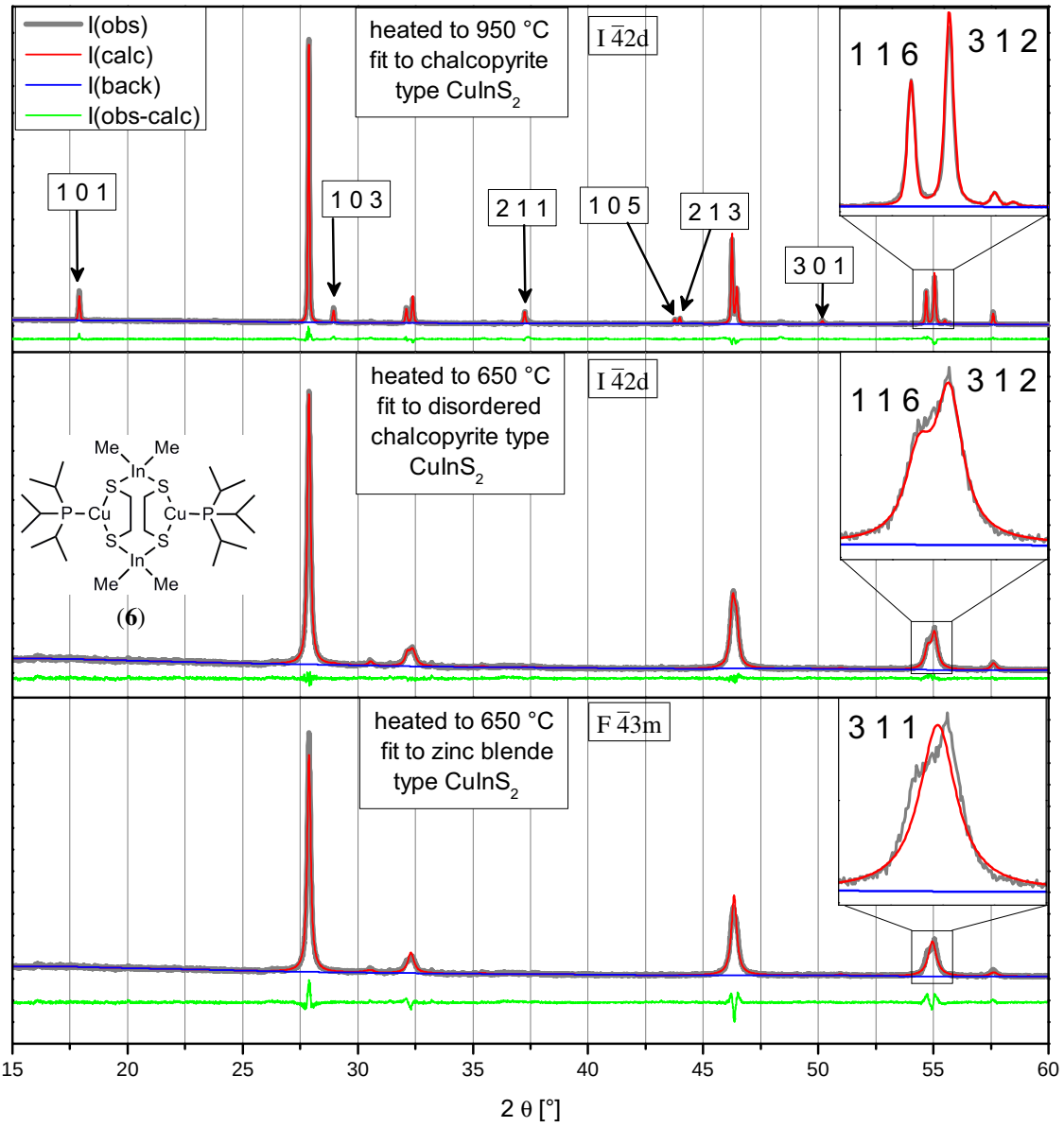

Fig. S 8 Rietveld refinements performed with PXRD data (Cu-$K_{\alpha 1}$) of thermolysis residues of $[(^{i}Pr_3PCu)_2(InMe)_2(SC_2H_4S)_2]$ **6**; **top:** residue was heated to 950 °C, fits to chalcopyrite type $CuInS_2$, marked reflections only appear when the thermolysis residue is heated to temperatures higher than 650 °C; **middle:** residue was heated to 650 °C, fit was performed with an metal ion disordered model of chalcopyrite type $CuInS_2$; **bottom:** same diffractogram as in middle, fit was performed with a metal ion disordered model of zinc blende type $CuInS_2$; Miller indices in zoom regions calculated for respective space group I $\bar{4}$2d or F $\bar{4}$3m.

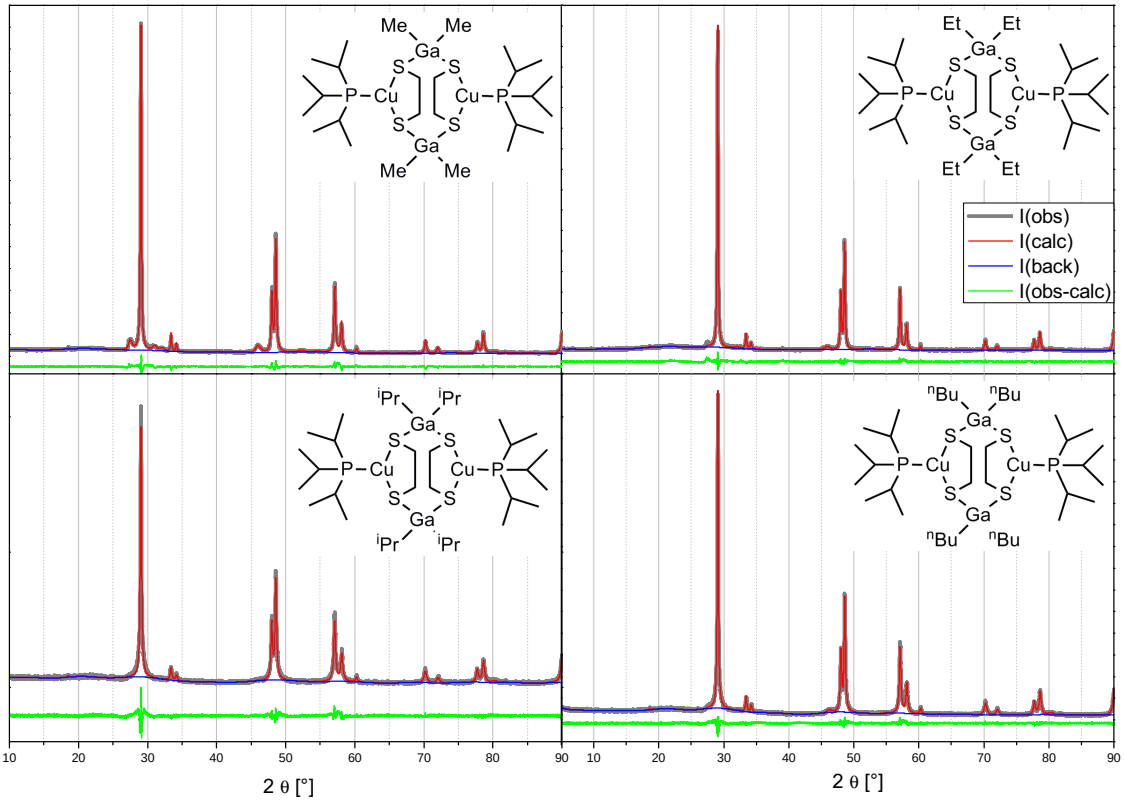

Residue compound	$CuGaS_2$	$Cu_{1.8}S$	Others %	RF^2 %	wR_p %	Δm %
$[(^iPr_3PCu)_2(GaR_2)_2(SCH_2CH_2S)_2]$						
Me **2**	78.81(5)	12.1(2)	9.1(2) [wurtzite]	2.43	5.88	60
Et **3**	90.12(3)	9.9(4)	-	2.46	7.14	58
^{i}Pr **4**	100	-	-	5.66	9.08	59
^{n}Bu **5**	96.653(9)	3.4(2)	-	1.80	5.45	60

Fig. S 9 Rietveld phase analysis of PXRD data of (Cu-$K_{\alpha 1}$) thermolysis residues (quartz tube experiment under N_2; 650 °C) of $[(^iPr_3PCu)_2(GaR_2)_2(SCH_2CH_2S)_2]$ (R = Me **2**, Et **3**, ^{i}Pr **4**, ^{n}Bu **5**), measured at room temperature.

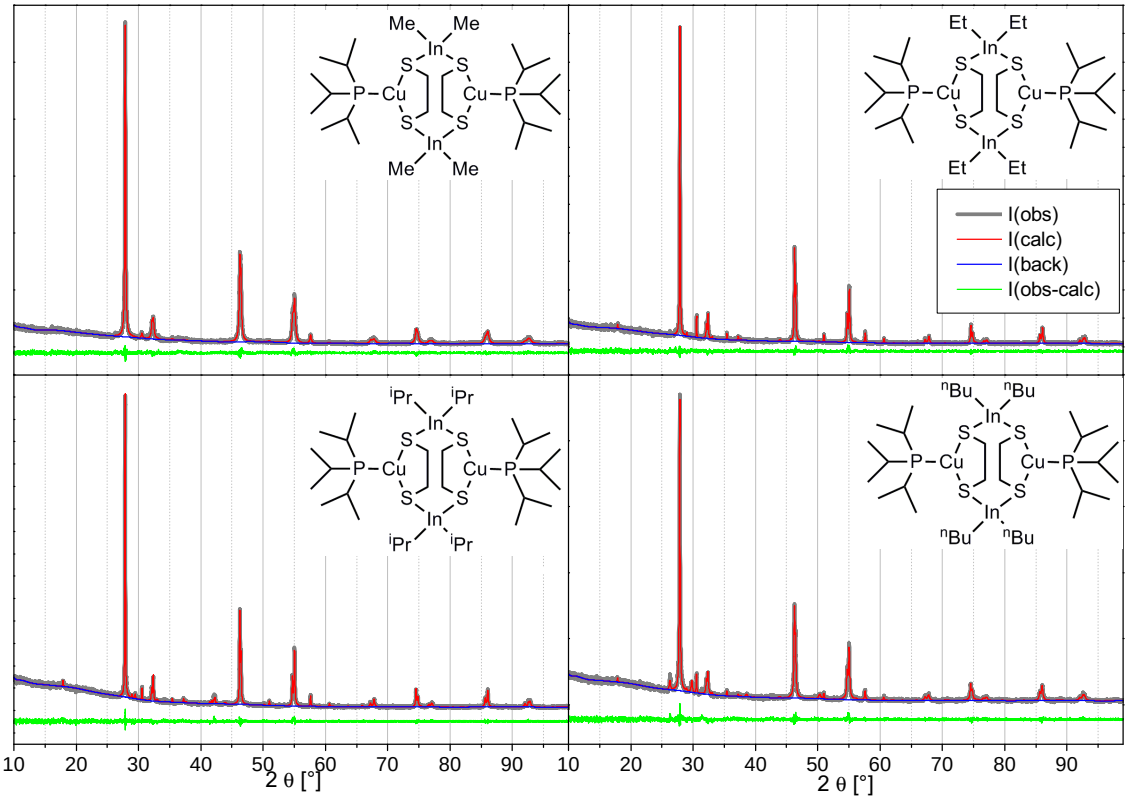

Residue compound	$CuInS_2$*	In_2O_3	Others	RF^2 %	wR_p %	Δm /%
$[(^iPr_3PCu)_2(InR_2)_2(SCH_2CH_2S)_2]$						
Me **6**	98.12(1) [60:40]	1.9(1)	-	8.49	8.22	51
Et **7**	95.87(2) [72:28]	4.1(1)	-	9.85	8.31	51
^{i}Pr **8**	92.27(3) [76:24]	2.5(1)	5.3(2) [$Cu_{11}In_9$]	8.65	6.71	55
^{n}Bu **9**	85.47(7) [70:30]	3.4(1)	11.1(3) [wurtztite]	7.31	8.04	56

Fig. S 10 Rietveld Phase analysis of PXRD data of (Cu-$K_{\alpha 1}$) of thermolysis residues (quartz tube experiment under N_2; 650 °C) of $[(^iPr_3PCu)_2(InR_2)_2(SCH_2CH_2S)_2]$ (R = Me **6**, Et **7**, ^{i}Pr **8**, ^{n}Bu **9**), measured at room temperature; *: The ratios given in brackets behind the w% -values give the distribution between original (left value) and inverse (right value) metal ion distribution in a disordered chalcopyrite $CuInS_2$ model.

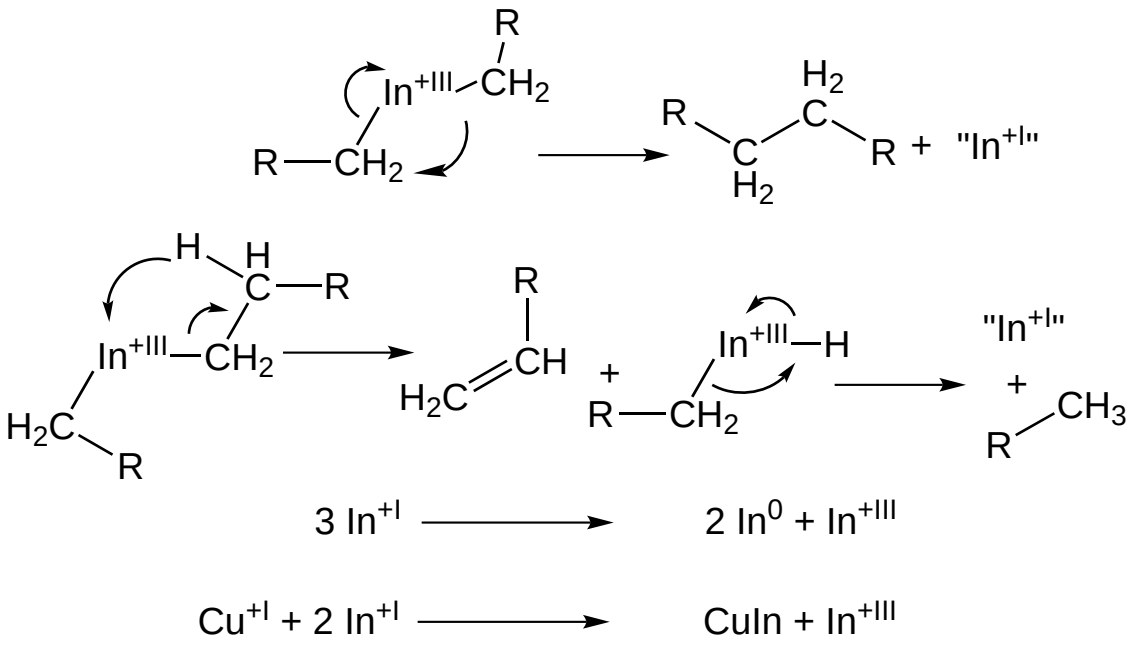

Fig. S 11 Possible pathways of reductive elimination reactions of alkylindium compounds

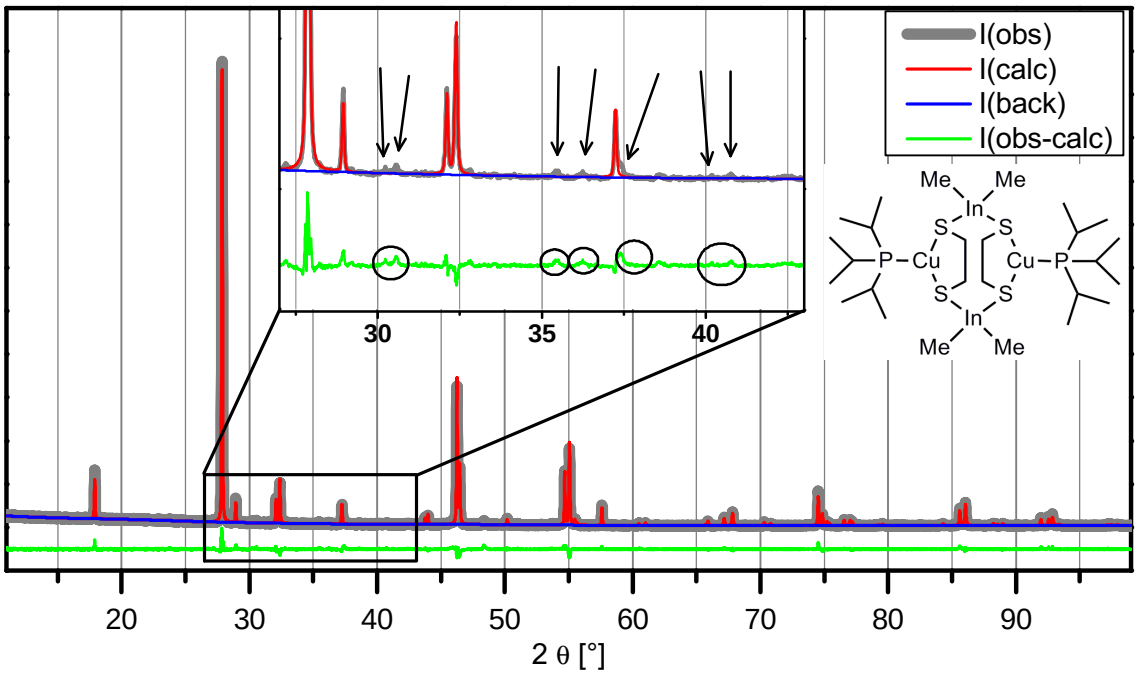

Fig. S 12 Proof of minor amounts of chalcocite Cu_2S [17] (marked by arrows in powder pattern and circles) in Rietveld plot of a thermolyis residue of $[(^iPr_3PCu)_2(InMe_2)_2(SCH_2CH_2S)_2]$ (**6**); residue was initially obtained by thermolysis at 650 °C in a quartz tube under N_2 atmosphere and then heated to 950 °C; powder X-ray pattern obtained at room temperature using Cu-$K_{\alpha 1}$ radiation.

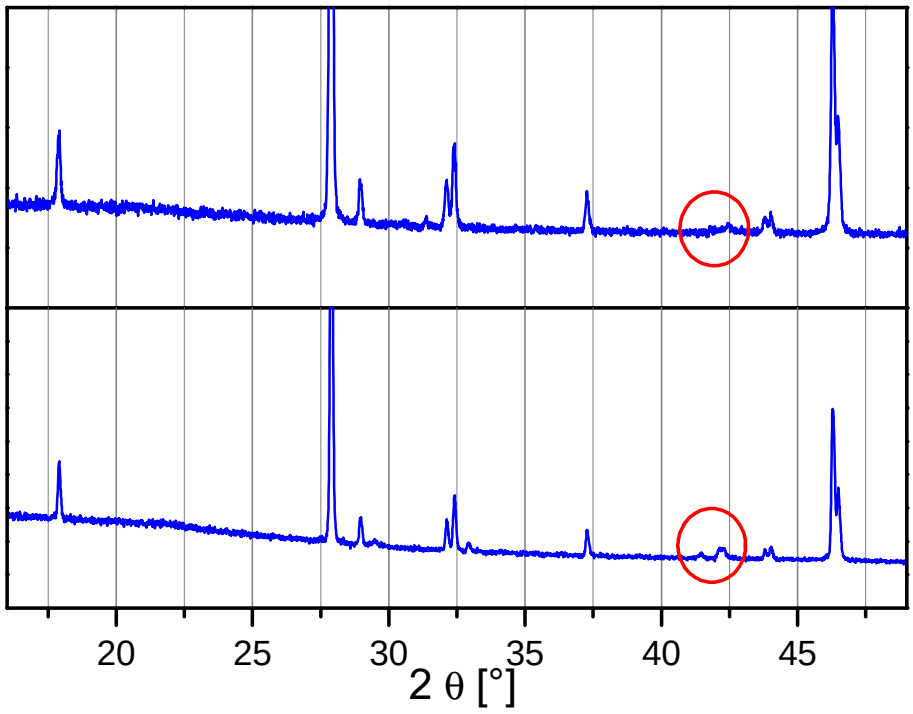

Fig. S 13 Proof of minor amounts of Cu_xIn_y phases [19,22,23] (marked by circles) in powder pattern of thermolyis residues of $[(^iPr_3PCu)_2(InEt_2)_2(SCH_2CH_2S)_2]$ (**7**) (top) and $[(^iPr_3PCu)_2(In^nBu_2)_2(SCH_2CH_2S)_2]$ (**9**) (bottom); residues were initially obtained by thermolysis at 650 °C in quartz tube under N_2 atmosphere and then heated to 950 °C; powder X-ray pattern obtained at room temperature using Cu-$K_{\alpha 1}$ radiation.

1.5 Thermolysis of complexes with Cu:M:S = 3:1:2

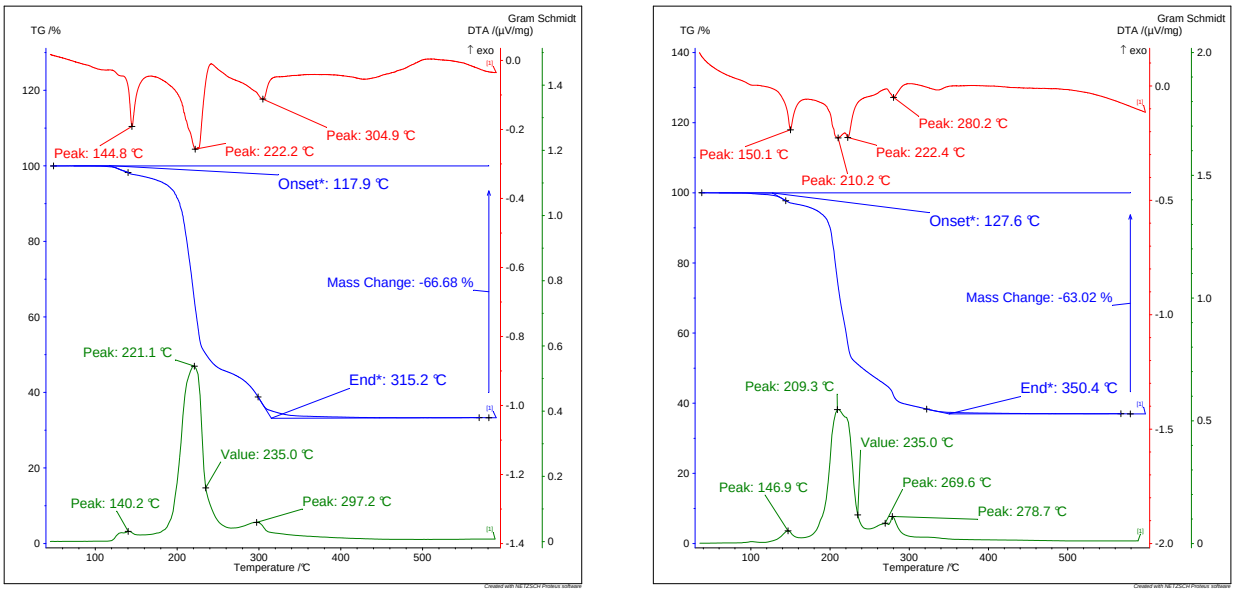

Fig. S 14 STA-results of [(^{i}Pr$_3$PCu)$_3$(SC$_2$H$_4$S)$_2$GaMe$_2$] (**10**) (left) and [(^{i}Pr$_3$PCu)$_3$(SC$_2$H$_4$S)$_2$InMe$_2$] (**14**) (right); blue: TG graph, green: Gram-Schmidt signal, red: DTA graph.

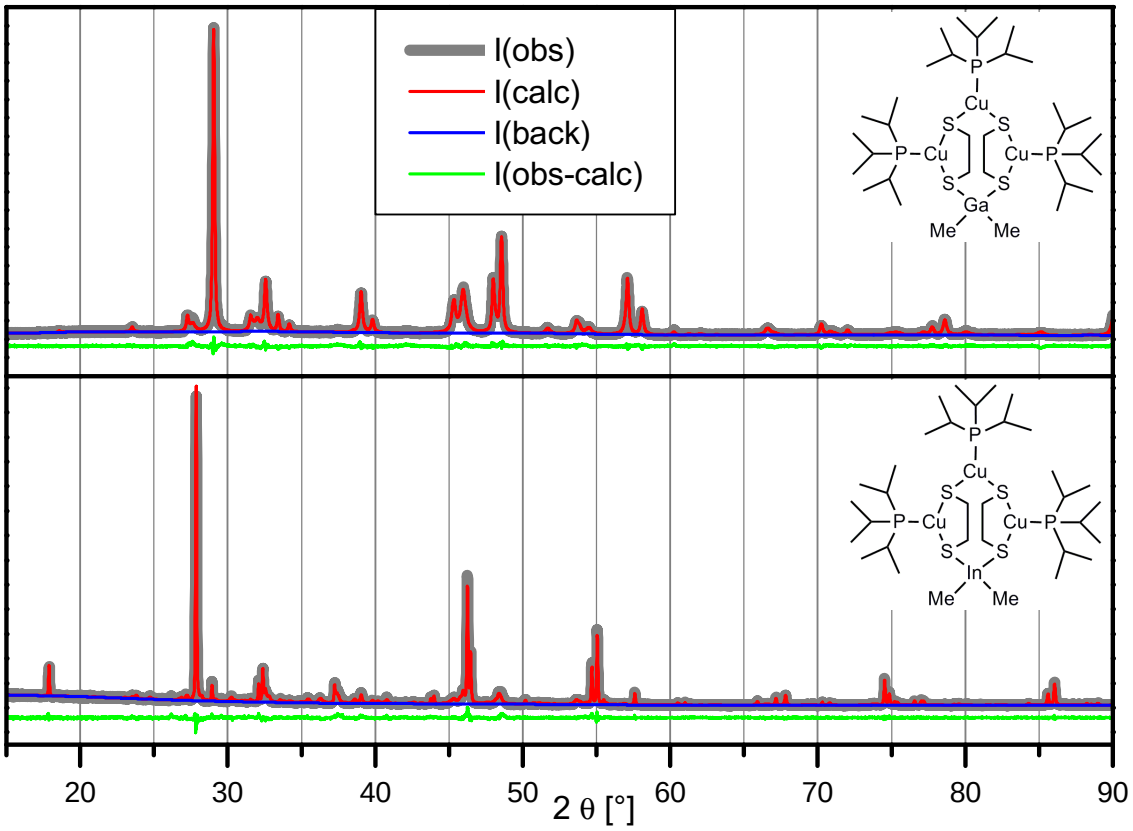

Residue compound	$CuMS_2$ /w%	$Cu_{1.8}S$ /w%	Cu_2S /w%	RF^2	wR_p /%	Δm /%
M = Ga (**10**)	40.24(8)	27.5(2)	32.3(1)	5.17	6.51	67
M = In (**14**)	42.5(1)		57.5(5)	11.31	8.30	64

Fig. S 15 Results of Rietveld refinements of thermolysis residues of $[(^iPr_3PCu)_3(GaMe_2)(SC_2H_4S)_2]$ (**10**) (top; TG experiment with heating till 600 °C) and $[(^iPr_3PCu)_3(InMe_2)(SC_2H_4S)_2]$ (**14**) (bottom; thermolysis at 950 °C in quartz tube under N_2 atmosphere); diffraction patterns collected at room temperature using Cu-$K_{\alpha 1}$ radiation.

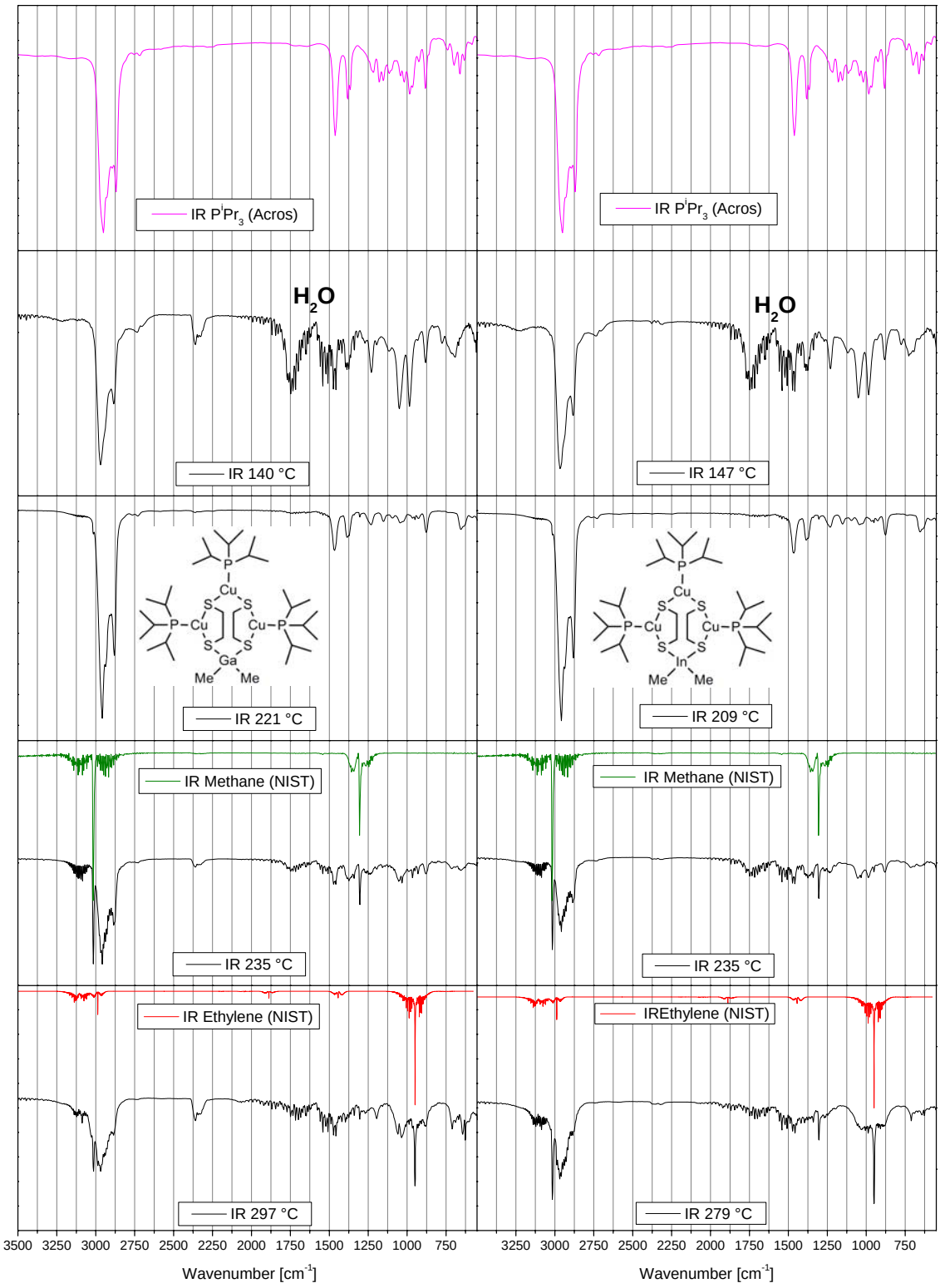

Fig. S 16 FTIR spectra of volatile thermolysis products recorded during STA experiments of [(^{i}Pr$_3$PCu)$_3$(MMe$_2$)(SC$_2$H$_4$S)$_2$] (M = Ga (**10**) (left side), In (**14**) (right side)) in comparison with reference spectra of P^{i}Pr$_3$, methane and ethene.

References

[1] STOE und Cie GmbH, *X-AREA*, 2006.

[2] L. J. Farrugia, *Journal of Applied Crystallography*, 1999, **32**, 837–838.

[3] G. M. Sheldrick, *Acta Cryst.*, 2008, **64**, 112–122.

[4] A. Altomare, G. Cascarano, C. Giacovazzo and A. Guagliardi, *J. Appl. Crystallogr.*, 1993, **26**, 343–350.

[5] K. Brandenburg, *Diamond*, 2010.

[6] *International tables for crystallography*, ed. T. Hahn and A. J. C. Wilson, Kluwer Academic Publishers, Dordrecht and Boston, 4th edn., 1996.

[7] STOE und Cie GmbH, *Win XPOW*, 2009.

[8] H. M. Rietveld, *Z. Kristallogr.*, 2010, **225**, 545–547.

[9] A. C. Larson and R. B. Dreele, *General Structure Analysis System (GSAS)*, 2004.

[10] B. H. Toby, *J. Appl. Crystallogr.*, 2001, **34**, 210–213.

[11] S. C. Abrahams and J. L. Bernstein, *J. Chem. Phys.*, 1973, **59**, 5415.

[12] H. Hahn, G. Frank, W. Klingler, A.-D. Meyer and G. Störger, *Z. Anorg. Allg. Chem.*, 1953, **271**, 153–170.

[13] O. Kluge, D. Friedrich, G. Wagner and H. Krautscheid, *Dalton Trans.*, 2012, **41**, 8635.

[14] Y. Qi, Q. Liu, K. Tang, Z. Liang, Z. Ren and X. Liu, *J. Phys. Chem. C*, 2009, **113**, 3939–3944.

[15] K. Yamamoto and S. Kashida, *J. Solid State Chem.*, 1991, **93**, 201–211.

[16] A. Janosi, *Acta Cryst.*, 1964, **17**, 311–312.

[17] H. T. Evans, *Z. Kristallogr.*, 1979, **150**, 299–320.

[18] W. H. Zachariasen, *Norsk Geologisk Tidsskrift*, 1927, **9**, 310–316.

[19] T. Rajasekharan and K. Schubert, *Z. Metallkd.*, 1981, **72**, 275–278.

[20] S.-H. Wei, S. B. Zhang and A. Zunger, *Phys. Rev. B*, 1999, **59**, R2478–R2481.

[21] D. S. Su and S.-H. Wei, *Appl. Phys. Lett.*, 1999, **74**, 2483.

[22] A. S. Koster, L. R. Wolff and G. J. Visser, *Acta Cryst.*, 1980, **B36**, 3094–3096.

[23] S. Lidin, L. Stenberg and M. Elding, *J. Alloy Compd.*, 1997, **255**, 221–226.